Modeling and Optimization of High-Frequency Ultrasound Transducers

Geoffrey R. Lockwood and F. Stuart Foster, *Member, IEEE*

Abstract—**Obtaining an accurate transducer model for a high-frequency transducer can be troublesome using traditional models, such as the KLM model, since it is often difficult to measure precisely the piezoelectric, dielectric, and mechanical properties of the transducer. This paper describes an alternative method of modeling transducers using network theory. The network theory model for a transducer is determined from a measurement of the transducer impedance in water and the pulse–echo response of the system for a given electrical source and load. A discussion of how this model can be used to optimize the design of an electrical matching circuit is given. This method is illustrated by designing a two-element transmission line matching circuit for a miniature 53 MHz transducer. Excellent agreement between the network model prediction and the experimental response is obtained.**

I. Introduction

NEW medical applications of B-mode ultrasound imaging such as endoluminal imaging [1], intravascular imaging [2], ocular imaging [3] and skin imaging [4], have created a need for miniature high-frequency ultrasound transducers. The miniature size (<3 mm diameter) and high frequency (20 MHz) of these transducers introduce a number of technical problems that are not encountered in the design of conventional 1–10 MHz medical ultrasound transducers. Traditional methods for minimizing the insertion loss and optimizing the pulse shape [5]–[7] are often ineffective due to nonideal element behavior, an imprecise knowledge of the electrical and mechanical properties of the system and the difficult in fabricating acoustic matching layers. Since acoustic matching is difficult, the design of an optimal electrical matching or tuning circuit is very important. Transducer models, such as the KLM model [8], which are used to design these matching circuits also rely on a precise knowledge of the electrical and mechanical properties of the transducer and can be quite inaccurate. Difficulty in modeling miniature or high-frequency transducers is an important obstacle limiting the development of these transducers.

This paper describes a method of modeling high-frequency ultrasound transducers using network theory. With this approach, the transducer is treated as a black box, and an equivalent model is derived from a set of measurements made at the input and output terminals of the transducer, without any knowledge of the properties of the transducer material or even the dimensions of the transducer. Once this model is determined, the pulse–echo response of the system can be calculated for any given configuration of the system. This permits the designer to accurately model different configurations of the system and to optimize the final design using a computer. An example is provided which illustrates the application of this model to optimize the design of a simple two-element transmission line matching network for a 2 mm diameter 53 MHz ceramic transducer.

Manuscript received July 13, 1993; revised September 15, 1993.

The authors are with Sunnybrook Health Science Center, Riechmann Research Building, Toronto, Ont. M4N 3M5, Canada.

IEEE Log Number 9214980.

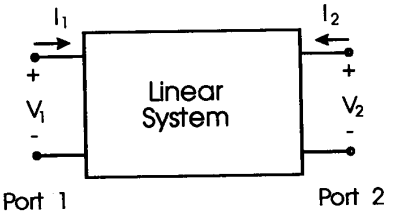

Fig. 1. A linear two-port network.

II. Derivation of a Network Transducer Model

Network theory is based on the principle that if a system is linear, then there exists a set of linear equations relating the input and output variables. For example, if we consider the linear two-port network shown in Fig. 1, and choose $I_1(\omega)$ and $I_2(\omega)$ as the independent variables, an impedance matrix relating the voltage at the input $V_1(\omega)$ and output $V_2(\omega)$ port to the current at each port can be defined.

Note: Capital letters will be assumed to represent frequency domain variables and for brevity the (ω) term will be dropped.

$$\begin{bmatrix} V_1 \\ V_2 \end{bmatrix} = \begin{bmatrix} Z_{11} & Z_{12} \\ Z_{21} & Z_{22} \end{bmatrix} \begin{bmatrix} I_1 \\ I_2 \end{bmatrix}. \tag{1}$$

By determining the elements of the matrix $(Z_{11}, Z_{12}, Z_{21}, Z_{22})$ the network can be completely specified and the output current or voltage can be calculated for any given source or load. The parameters of the matrix can be measured by applying a known current at one port with the other port open circuited and measuring the voltage at each port. For instance, if port 2 is open circuited then $I_2 = 0$ and it follows from (1) that

$$Z_{11} = \frac{V_1}{I_1} \tag{2}$$

$$Z_{21} = \frac{V_2}{I_1}. \tag{3}$$

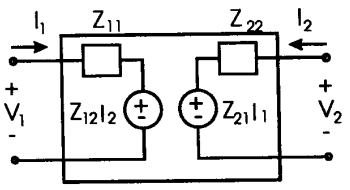

Fig. 2. Equivalent circuit representation of a linear two-port network. The variables are defined in (2)–(4).

Similarly if port 1 is open circuited then $I_1 = 0$ and

$$Z_{12} = \frac{V_1}{I_2} \tag{4}$$

$$Z_{22} = \frac{V_2}{I_2}. \tag{5}$$

An equivalent circuit representation of the impedance matrix consists of two impedance terms and two current dependent voltage sources and is shown in Fig. 2. This ability to describe any linear network by a simple arrangement of four circuit elements provides a useful method for modeling a complex system. A detailed description of network theory is given by Roe [9].

The basic ideas that have just been introduced can be applied to derive a network representation of a transducer. When the same transducer is used to transmit and receive the acoustic energy, the input impedance Z_{11} and output impedance Z_{22} of the equivalent network model will be identical and will be given by the electrical impedance of the transducer Z_{IN}. This can be measured directly using an impedance analyzer.

$$Z_{\mathrm{IN}} = Z_{11} = Z_{22} \tag{6}$$

The remaining network parameters Z_{12} and Z_{21} cannot be measured directly but can be calculated by exciting the transducer with a known electrical source (voltage V_S, impedance Z_S) and measuring the response of the system (V_L) across a given electrical load (Z_L) as shown in Fig. 3. From these measurements, the current and voltage at each port of the transducer can be calculated.

$$V_1 = V_S \frac{Z_{\mathrm{IN}}}{Z_{\mathrm{IN}} + Z_S} \tag{7}$$

$$I_1 = \frac{V_S}{Z_{\mathrm{IN}} + Z_S} \tag{8}$$

$$V_2 = V_L \tag{9}$$

$$I_2 = -\frac{V_L}{Z_L}. \tag{10}$$

Substituting (7)–(10) into (1) and solving for Z_{12} and Z_{21}, we find

$$Z_{12} = \frac{V_1 - Z_{11}I_1}{I_2} = 0 \tag{11}$$

and

$$Z_{21} = \frac{V_2 - Z_{22}I_2}{I_1} = \frac{V_L}{V_S}(Z_{22} + Z_S)\left(1 + \frac{Z_{22}}{Z_L}\right). \tag{12}$$

The open circuit voltage transfer function (γ = open circuit output voltage/input voltage) can be related to the network

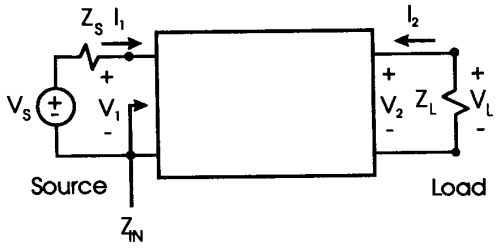

Fig. 3. Circuit for deriving the network parameters for a transducer. The transducer is excited with an electrical source (voltage V_S, impedance Z_S) and the received pulse–echo response is recorded across an electrical load (impedance Z_L).

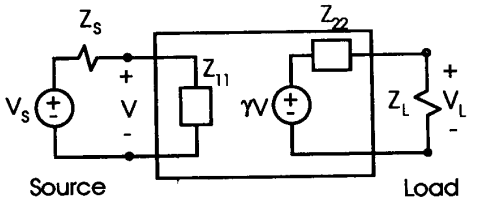

Fig. 4. Equivalent electrical circuit for the transducer. Z_{11} is the electrical input impedance, Z_{22} is the electrical output impedance and γ is the open circuit transfer function of the transducer.

parameters and is given by the expression

$$\gamma = \frac{Z_{21}}{Z_{11}} \tag{13}$$

The equivalent network model of the transducer is shown in Fig. 4.

In practice, calculating the network parameters for a transducer based on an experimental measurement of the response of the system is complicated by the need to simultaneously couple the transducer to both the pulsing electronics and the receiving electronics. During the transmit part of the pulse–echo sequence, the receiver amplifiers must be protected from the high source voltage. As well, during the receive part of the sequence it is desirable to remove the high voltage source from the circuit to eliminate noise from the pulser electronics. The most common solution to this problem employs crossed diode bridges (Fig. 5). One pair of crossed diodes is placed in series with the output of the pulser (referred to as an expander) while the other pair is placed in parallel with the input of the amplifier (referred to as a limiter). During the large excitation pulse, all the diodes will conduct creating a clear path from the pulser to the T junction but a short circuit at the input of the receiver amplifier. By selecting a line length of one quarter of a wavelength ($\lambda/4$) between the T junction and the receiver amplifier, the short circuit at the amplifier will look like an open circuit at the T junction and the amplifier will have been switched out of the circuit. After the large excitation pulse has passed, the diode bridges will become open circuits which switch the pulser out of the circuit but leave a clear path to the amplifier. The $\lambda/4$ line no longer has any effect provided that the input impedance of the amplifier is matched to the line impedance. In a broad-band system, the $\lambda/4$ line

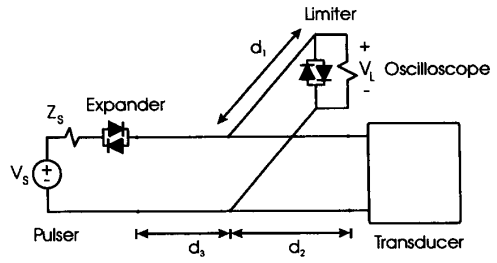

Fig. 5. Configuration of the pulser, transducer, load (oscilloscope), and protection circuit.

will only be the correct length for a single frequency. At other frequencies, the $\lambda/4$ line will introduce an impedance which is frequency and line length dependent. In addition, the lines connecting the transducer and the pulser to the T junction will also introduce impedance terms unless the length of these lines is kept much smaller than a wavelength. Careful selection of these lines is important to obtain the optimal response of the system [10].

The presence of the protection circuit can be most easily included in the network model by replacing the source and load [in (12)] by their Thevenin equivalents, measured after the protection circuit. It is important that experimental measurements of the transducer, the source and the load all be made from the same location in the system under the appropriate circuit conditions. The source is measured with the two pairs of crossed diodes replaced by short circuits, while the load impedance is measured with the diodes replaced by open circuits. It is convenient to make these measurements at the T junction since in this case, the calculated response of the system (V_L') will be identical, with the exception of a phase shift, to the response that would be measured by the receiver amplifier (V_L). The configuration of the circuits for measuring the Thevenin equivalent of the source (V_S', Z_S'), load (Z_L') and transducer (Z_{IN}') are shown in Fig. 6. Once these measurements are made, the network parameters can be calculated by simply substituting V_S', Z_S', V_L', Z_L', and Z_{IN}' for V_S, Z_S, V_L, Z_L, and Z_{IN} in (6) and (12).

III. Computer Optimization Using the Network Model

The network model which was introduced in Section II provides an accurate way of modeling the transducer. This section gives a discussion of how the network model can be used in a computer program to optimize the design of a matching circuit.

A number of researchers have investigated the design of matching circuits for piezoelectric transducers [5]–[7]. The goal of these designs is to minimize the insertion loss of the system over the largest possible bandwidth. A very effective technique for obtaining this goal was introduced by Selfridge *et al.* [11] who suggested that optimal performance of a system can most easily be determined in the time domain by calculating the pulse echo response of the system ($v_L(t)$). The pulse echo response is then used to determine a "badness

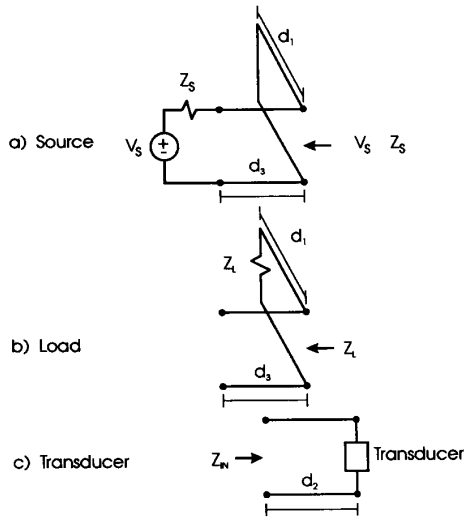

Fig. 6. Circuits for measuring the (a) source (pulser) impedance and voltage, (b) load (oscilloscope) impedance, and (c) transducer electrical impedance.

criteria" which is defined by the following function:

$$\text{"badness"} = \frac{\int_{t_0}^{\infty} |v_L(t)|(t - t_0)\, dt}{s^2} \tag{15}$$

where s is the peak amplitude of the pulse echo response and t_0 is the time of the fifth zero crossing in the pulse echo response. By adjusting the values of elements in a matching circuit to minimize the "badness" function, the optimal response [maximum amplitude and minimum pulse length as defined by (15)] of the system is obtained.

If the configuration of the system is known and will not be varied, an analytical expression for the pulse–echo response can be calculated from the network (Fig. 4) using standard circuit analysis. Unfortunately, this analytical expression quickly becomes extremely complicated if more than a few matching elements are used. If an optimization program is to be used to investigate more than one circuit configuration, an analytical expression for the response of the system must first be derived for each configuration. The effort required to derive this expression for different configurations of a multielement matching circuit could easily become prohibitive. This problem can be simplified by transforming the impedance network parameters ($Z_{11}, Z_{12}, Z_{21}, Z_{22}$), representing the transducer, to a second equivalent set of network parameters called the $ABCD$ parameters.

$ABCD$ parameters are defined by the matrix (16) which relates the voltage and current at the input port of a linear two-port network to the voltage and current at the

$$\begin{bmatrix} V_1 \\ I_1 \end{bmatrix} = \begin{bmatrix} A & B \\ C & D \end{bmatrix} \begin{bmatrix} V_2 \\ -I_2 \end{bmatrix} \tag{16}$$

output port of the network. By representing not only the transducer but also each element in the system by an individual $ABCD$ parameter two-port network, the problem of calculating the pulse echo response of the system can be reduced to a

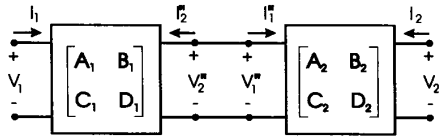

Fig. 7. Cascaded two-port networks representing two cascaded circuit elements.

series of matrix multiplications. This property of the $ABCD$ parameters can be derived from the matrix which defines the parameters. If two $ABCD$ networks are cascaded (Fig. 7) then the voltage (V_2) and current (I_2) at the output of the first network will be identical to the voltage (V_1) and current (I_1) at the input of the second network and the two matrices can be represented by a single matrix given by their product.

$$\begin{bmatrix} V_1 \\ I_1 \end{bmatrix} = \begin{bmatrix} A_1 & B_1 \\ C_1 & D_1 \end{bmatrix} \begin{bmatrix} A_2 & B_2 \\ C_2 & D_2 \end{bmatrix} \begin{bmatrix} V_2 \\ -I_2 \end{bmatrix}. \tag{17}$$

It follows that a single two-port network representing the entire system can be found from the product of the matrices representing individual elements. This considerable simplifies the problem of evaluating different configurations of the system. For instance, elements can be added, removed or changed by simply adding, removing, or changing the appropriate matrix. It is for this reason that it is convenient to transform the impedance network parameters representing the transducer to equivalent $ABCD$ network parameters. This transformation can be derived from (1) and (16) and is given below [9]

$$A = \frac{Z_{11}}{Z_{21}}, B = \frac{Z_{11}Z_{22} - Z_{12}Z_{21}}{Z_{21}},$$
$$C = \frac{1}{Z_{21}}, D = \frac{Z_{22}}{Z_{21}}. \tag{18}$$

Note: it would have been possible to derive the $ABCD$ network parameters for a transducer directly from (16) in an analogous manner to what was done in Section II, however, this derivation is more involved and the resulting model does not lend itself to interpretation as an equivalent circuit.

The $ABCD$ matrix for any circuit element can be derived from (16). Examples of the $ABCD$ matrix for a parallel circuit element (Z_P), a series circuit element (Z_S) a series transmission line (length d, impedance Z_0, transmission constant $\beta = 2\pi/\lambda$) and a parallel open circuit transmission line (d, Z_0, β) are given in (19), (20), (21), and (22), respectively.

$$\begin{bmatrix} 1 & 0 \\ 1/Z_P & 1 \end{bmatrix} \tag{19}$$

$$\begin{bmatrix} 1 & Z_S \\ 0 & 1 \end{bmatrix} \tag{20}$$

$$\begin{bmatrix} \cosh \beta d & Z_0 \sinh \beta d \\ 1/Z_0 \sinh \beta d & \cosh \beta d \end{bmatrix} \tag{21}$$

$$\begin{bmatrix} 1 & 0 \\ \frac{\tanh \beta d}{Z_0} & 1 \end{bmatrix}. \tag{22}$$

The use of $ABCD$ parameters with the transducer network model permits the development of a relatively simple and flexible computer program for optimizing the design of the system. This is illustrated in the following example which considers the design of a simple two-element transmission line matching circuit.

IV. Transmission Line Matching Example

To illustrate an application of the network model to electrical matching, the network model was derived for a 2 mm diameter 53 MHz PZT transducer. A detailed description of this transducer is provided in a companion paper [12]. The transducer was excited with a 17 V monocycle pulse produced by an Avtech pulser (Avtech, Ottawa, Canada, model AVB2-CO) and the pulse–echo response (V_L), from a quartz reflector placed at the focal region of the transducer, was recorded using a 300 MHz digital oscilloscope (Hewlett Packard, Palo Alto, CA, model 54201D). The transducer, pulser and oscilloscope were connected using the protection circuit show in Fig. 5 with $d_1 = 52$ cm, $d_2 = 25$ cm, and $d_3 = 5$ cm. The source voltage (V_S') and impedance (Z_S') and the load impedance (Z_L') were also measured as show in Fig. 6. The electrical input impedance of the transducer (Z_{IN}') with a water acoustic load was measured over the frequency range from 1 to 100 MHz in steps of 1 MHz using an RF impedance analyzer (Hewlett-Packard, Palo Alto, CA, model 4191A). Once there measurements were made, the network parameters were calculated using (6) and (12) and transformed into $ABCD$ parameters using (18). The $ABCD$ network parameters representing the transducer were then used in a computer program to optimize the design of a two element transmission line matching circuit.

The configuration of the transmission line matching circuit is shown in Fig. 8. The matching circuit consists of a parallel open circuit stub and a series transmission line. The circuit is placed at the transducer side of the T junction and therefore appears on both the transmit and receive side of the model (Fig. 8). The relationship between the current and voltage at the input and output of the system is calculated from the product of $ABCD$ matrices representing each element

$$\begin{bmatrix} V_S \\ I_S \end{bmatrix} = \begin{bmatrix} A' & B' \\ C' & D' \end{bmatrix} \begin{bmatrix} V_L \\ -I_L \end{bmatrix} \tag{23}$$

where

$$\begin{bmatrix} A' & B' \\ C' & D' \end{bmatrix} = \begin{bmatrix} 1 & Z_S \\ 0 & 1 \end{bmatrix} \begin{bmatrix} \cosh \beta l_B & Z_0 \sinh \beta l_B \\ \frac{\sinh \beta l_B}{Z_0} & \cosh \beta l_B \end{bmatrix} \cdot \begin{bmatrix} 1 & 0 \\ \frac{\tanh \beta l_A}{Z_0} & 1 \end{bmatrix} \cdot \begin{bmatrix} A & B \\ C & D \end{bmatrix} \begin{bmatrix} 1 & 0 \\ \frac{\tanh \beta l_A}{Z_0} & 1 \end{bmatrix} \cdot \begin{bmatrix} \cosh \beta l_B & Z_0 \sinh \beta l_B \\ \frac{\sinh \beta l_B}{Z_0} & \cosh \beta l_B \end{bmatrix} \begin{bmatrix} 1 & 0 \\ 1/Z_L & 1 \end{bmatrix}. \tag{24}$$

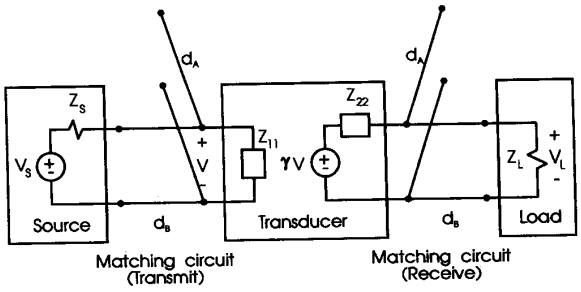

Fig. 8. Configuration of the two-element transmission line matching circuit. The length of each transmission line (d_A, d_B) is varied to optimize the pulse–echo response.

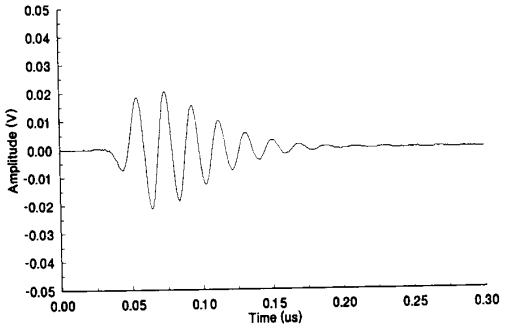

Fig. 9. Experimental pulse–echo response prior to matching.

Substituting $I_L = -V_L/Z_L$ into (23) and solving for V_L, we find

$$V_L = \frac{V_S}{A' + B'/Z_L} \tag{25}$$

The pulse–echo response of the system $(v_L(t))$ is calculated from the inverse Fourier transform of the load spectrum (V_L).

The design of the transmission line matching circuit (Fig. 8) was optimized by varying the length of each transmission line and calculating the pulse–echo response. A figure of merit for each design was then calculated using the "badness" function (15); the best design being the one with the minimum "badness." Each transmission line in the matching circuit was varied from 5 to 195 cm in steps of 10 cm. The optimal design $(d_A = 45$ cm, $d_B = 145$ cm) was found after a computation time of approximately 100 s using an IBM compatible 486 computer.

The pulse–echo response of the system prior to matching is shown in Fig. 9. The theoretical and experimental pulse–echo response following matching are shown in Fig. 10. Compared to the unmatched case (Fig. 9), there is a 2.4 times increase in amplitude of the pulse–echo response. The pulse spectra for the transducer before and after matching are shown in Fig. 11. The pulse has a center frequency of 53 MHz and a 6 dB bandwidth of approximately 24% before matching and 30% after matching. There is excellent agreement between the network model prediction and the experimental response.

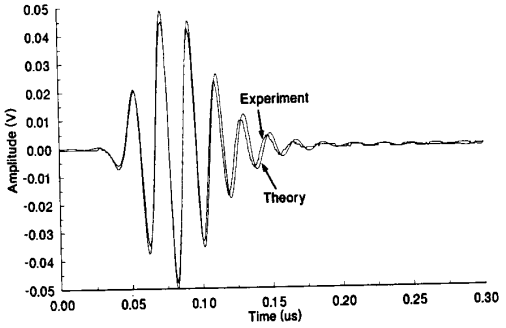

Fig. 10. Theoretical and experimental pulse–echo response following matching. The amplitude of the response following matching is increased by 2.4 times.

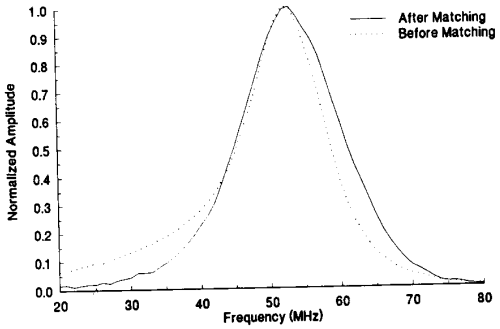

Fig. 11. Pulse spectrum before and after matching. The 6 dB bandwidth of the pulse is 24% prior to matching and 30% following matching.

V. Summary and Conclusion

This paper described a new method for modeling transducers based on network theory. The major advantage of this model over conventional models, such as the KLM model, is that the network model can be derived from measurements at the electrical port of the transducer, without any knowledge of the piezoelectric, dielectric, or mechanical properties of the transducer. This is an important advantage when modeling high frequency of miniature transducers where precise knowledge of these properties may be unavailable. Since the model is derived from experimental measurements, frequency dependent losses and nonideal element behavior are easily taken into account.

$ABCD$ parameters were introduced to facilitate the development of a numerical optimization program for designing the system. By using $ABCD$ parameters, different configurations of the system can be investigated by simply inserting or changing the appropriate $ABCD$ matrix. An example was given in which a two-element transmission line matching circuit was designed to optimize the response (maximum amplitude and bandwidth) of a 53 MHz PZT transducer. The matching circuit increased the amplitude of the pulse by more than two times and improved the 6 dB bandwidth from 24 to 30%. More importantly, this example demonstrated the

excellent accuracy with which the network model was able to predict the experimental pulse–echo response of the system.

REFERENCES

[1] N. T. Sanghvi, M. Wiersema, C. R. Reilly, P. E. Smith, and T. D. Franklin, "PC based high resolution, high frequency US system for gastroenterology," in *Proc. IEEE Ultrason. Symp.*, 1990, pp. 1477–1479.

[2] J. McB. Hodgson, S. P. Graham, A. D. Savakus, S. G. Dame, D. N. Stephens, P. S. Dhillon, D. Brands, H. Sheehan, and M. J. Eberle, "Clinical percutaneous imaging of coronary anatomy using an over-the-wire ultrasound catheter system," *Int. J. Card. Imaging*, vol. 4, pp. 187–193, 1989.

[3] C. J. Pavlin, H. Harasiewicsz, M. D. Sherar, and F. S. Foster, "Clinical use of ultrasound biomicroscopy," *Ophthalmology*, vol. 98, pp. 287–295, 1991.

[4] F. K. Forster, J. E. Olerud, G. R. Pomajevich, A. W. Holms, and S. R. Sharer, "High frequency ultrasonic imaging and backscatter attenuation techniques for determination of thermal injury to skin," in *Proc. IEEE Ultrason. Symp.*, 1986, pp. 845–848.

[5] C. S. Desilets, J. D. Fraser, and G. S. Kino, "The design of efficient broad-band piezoelectric transducers," *IEEE Trans. Son. Ultrason.*, vol. SU-25, pp. 115–125, 1978.

[6] J. Anderson and L. Wilkins, "The design of optimum lumped broadband equalizers for ultrasound transducers," in *Proc. IEEE Ultrason. Symp.*, 1977, pp. 422–427.

[7] C. H. Chou, J. E. Bowers, A. R. Selfridge, B. T. Khuri-Yakub, and G. S. Kino, "The design of broadband and efficient acoustic wave transducers," in *Proc. IEEE Ultrason. Symp.*, 1980, pp. 984–988.

[8] D. Leedom, R. Krimholz, and G. Matthaei, "Equivalent circuits for transducers having arbitrary even-or-odd symmetry piezoelectric excitation," *IEEE Trans. Son. Ultrason.*, vol. SU-18, pp. 128–141, 1971.

[9] P. H. Roe, *Networks and Systems*. Reading, MA: Addison-Wesley, 1966, ch. 4.

[10] G. R. Lockwood, J. W. Hunt, and F. S. Foster, "The design of protection circuitry for high frequency ultrasound imaging systems," *IEEE Trans. Ultrason. Ferroelec. Freq. Contr.*, vol. 38, pp. 48–55, 1991.

[11] A. R. Selfridge, R. Baer, B. T. Khuri-Yakub, and G. S. Kino, "Computer-optimized design of quarter-wave acoustic matching and electrical matching networks for acoustic transducers," in *Proc. IEEE Ultrason. Symp.*, 1981, pp. 644–648.

[12] G. R. Lockwood, D. H. Turnbull, and F. S. Foster, "Fabrication of high frequency spherically shaped ceramic transducers," *IEEE Trans. Ultrason. Ferroelec. Freq. Contr.*, see this issue, pp. 231–235.

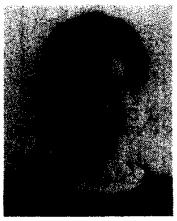

Geoffrey R. Lockwood was born in Toronto, Ont., Canada, on September 14, 1961. He received the B.A.Sc. degree in electrical engineering from the University of Toronto, Toronto, Ont., Canada, in 1985, and the M.Sc. and Ph.D. degrees in medical biophysics at the University of Toronto in 1988 and 1992, respectively.

He is presently a postdoctoral fellow with the Department of Medical Biophysics at the University of Toronto where he is working on the development of high-frequency ultrasound systems for medical imaging.

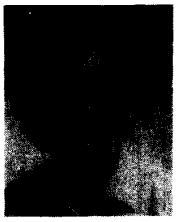

F. Stuart Foster (M'91) was born in Montreal, PQ, Canada, on July 29, 1951. He received the B.A.Sc. degree in engineering physics in 1974 from the University of British Columbia, Vancouver, BC, Canada, in 1974, and the M.Sc. and Ph.D. degrees in medical biophysics in 1977 and 1980, respectively, from the University of Toronto, Toronto, Ont., Canada.

He is presently a Senior Scientist with the Sunnybrook Health Science Centre, a senior Research Scholar of the National Cancer Institute of Canada, and a Professor of Medical Biophysics at the University of Toronto. He was a Senior Scientist with the Ontario Cancer Institute from 1980 to 1991. He has been involved with the development of conical and annular array transducers, ultrasound backscatter microscopy, and tissue characterization and more recently, in two-dimensional array technology and intravascular imaging.

Dr. Foster has twice won the Ultrasound in Medicine and Biology Prize and is on the editorial boards of Ultrasonic Imaging and Ultrasound in Medicine and Biology.